CFD Laboratory 3
Development of boundary layer over a flat plate

Sergio M. Vanegas A.
Francesco de Pas
Department of Mathematics
Polimi—Politecnico di Milano
Milano, Italia

December 4, 2021

Abstract

The present case concerns the development of the boundary layer produced by a uniform flow over a flat plate. The flow develops from a condition of uniform velocity U_∞ imposed at the inlet boundary, growing indefinitely without reaching a fully-developed state. Up to a distance x_{lam} from the leading edge such that $\mathrm{Re}_x = U_\infty x_{\mathrm{lam}}/\nu \approx 1 \times 10^5$, the boundary layer remains laminar; beyond a distance x_{turb} from the leading edge such that $\mathrm{Re}_x = U_\infty x_{\mathrm{turb}}/\nu \approx 3 \times 10^6$, the boundary layer is fully turbulent; in-between x_{lam} and x_{turb}, transitional boundary layer will occur. In this Laboratory, PHOENICS is used to simulate the development of the laminar boundary layer, whereas the analysis of the turbulent part will be shelved for further individual study. [1]
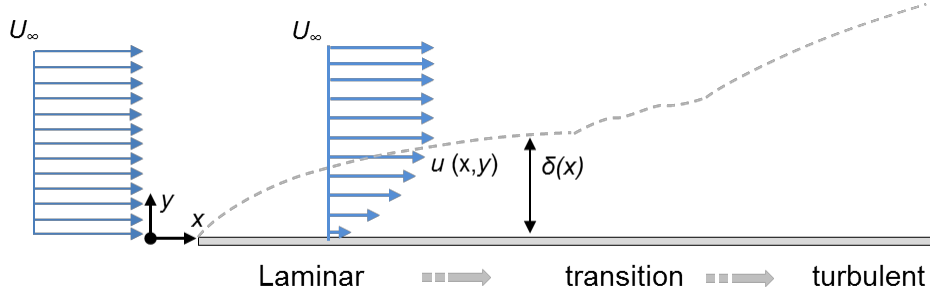
Figure 1: Sketch of the test case

1 Introduction

1.1 Reference Solution: Laminar Boundary Layer

Up to a distance from the leading edge x_{lam}, corresponding to $U_\infty x_{\mathrm{lam}}/\nu \approx 1E5$, a reference semi-analytical solution was obtained by Blasius. This solution expresses the fluid dynamic characteristics of the boundary layer as a function of the dimensionless parameter $\eta = y\sqrt{\frac{U_\infty}{\nu x}}$, as follows:

- U-velocity
$$\frac{u}{U_\infty} = f'(\eta)$$

- V-velocity
$$\frac{nu}{U_\infty}\sqrt{\frac{U_\infty x}{\eta}} = \frac{1}{2}\left[\eta f'(\eta) - f(\eta)\right]$$

From Blasius' solution, it is also possible to obtain the following other parameters:

- Wall shear-stress
$$\tau_w(x) = 0.332\rho U_\infty^2 \mathrm{Re}_x^{-\frac{1}{2}}$$

- Skin-friction coefficient
$$C_f(x) = \frac{\tau_w(x)}{\frac{1}{2}\rho U_\infty^2} = 0.664\mathrm{Re}_x^{-\frac{1}{2}}$$

- Boundary layer thickness based on the condition $0.99 U_\infty$

$$\frac{\delta(x)}{x} = 5\mathrm{Re}_x^{-\frac{1}{2}}$$

- Displacement thickness

$$\frac{\delta^*(x)}{x} = \frac{\int_0^\infty \left(1 - \frac{u}{U_\infty}\right) dy}{x} = 1.7208 \mathrm{Re}_x^{-\frac{1}{2}}$$

- Momentum thickness

$$\frac{\Theta^*(x)}{x} = \frac{\int_0^\infty \frac{u}{U_\infty}\left(1 - \frac{u}{U_\infty}\right) dy}{x} = 0.664 \mathrm{Re}_x^{-\frac{1}{2}}$$

1.2   Flow Domain

A possible sketch of the computational domain is shown in Figure 2. As for the earlier test cases, the inlet should not be placed in direct contact with the plate to avoid numerical issues at the bottom-left corner.
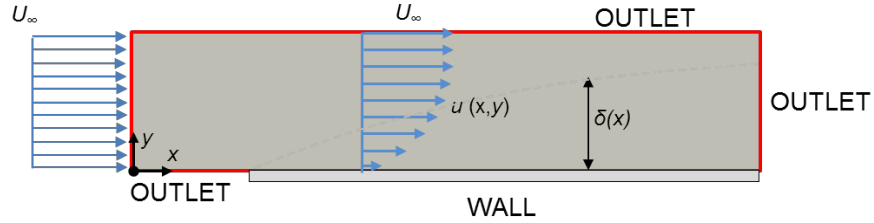

Figure 2: Computational domain and Boundary Conditions

Since the attention is restricted to the laminar boundary layer, the steady-state formulation of the Navier-Stokes equations can be solved. When defining the CFD model particular attention must be paid in choosing the proper boundary conditions, which are, in this case, inlet, outlet, solid walls and symmetry. Let us assume no gravity. Since the flow is incompressible, gravity does not have a direct effect on the velocity field, but it just brings about a hydrostatic contribution to the pressure field.

- At the inlet, a uniform x-velocity profile equal to U_∞ is imposed, whereas the y and z velocity components are specified as zero.

- At the outlet boundaries, a zero external p is imposed. Note that the value of p at the outlet will not be zero owing to the presence of a finite outlet coefficient. In order to have $p_\text{outlet} = p_\text{ext} = 0$, set the outlet coefficient to a very large value (e.g. 1×10^{10}). This is not really necessary though.

- At the solid wall, owing to the no-slip condition, the fluid velocity is zero. In the Finite Volume Framework with staggered-grid arrangement, only the y-velocity at the wall is imposed. The no-slip condition is imposed for the x-velocity indirectly. On the one hand, the advection flux of variable u through the near-wall cell faces is set to zero. On the other hand, the diffusion flux of variable u through the near-wall cell faces (that is, the wall shear-force) is specified by obtaining the wall shear-stress from the laminar friction coefficient.

1.3 configuration of the problem

- Free-stream velocity is $U_\infty = 1\,\mathrm{m\,s^{-1}}$

- Workinf fluid is air at $2 \times 10^1\,°\mathrm{C}$, treated as incompressible
  ($\rho = 1.189\,\mathrm{kg\,m^{-3}}, \nu = 1.5445 \times 10^{-5}\,\mathrm{m^2\,s^{-1}}$)

1.4 Document Structure

The remainder of the report is organized as follows: Section 2 addresses the general procedure of simulation convergence verification and mesh suitability, whereas Section 3 compares the simulation results against the reference model.

2 Suitability of the CFD model

In order to keep the flow within the Laminar BL, we set a domain length of $L = \frac{1 \times 10^5 \nu}{U_\infty} = 1.5445\,\mathrm{m}$ (with an additional $1 \times 10^{-1}\,\mathrm{m}$ at the beginning for computational padding). The channel height was instead qualitatively reduced until just a relatively small padding remained between the observable

limit of the boundary layer and the top of the domain; the resulting height was of 5×10^{-2} m.

Since pressure was not a variable of interest for this test case, its grid independence was not studied; in its stead, both the x and y-velocity profiles at the penultimate cell were analyzed for different cell configurations, resulting in the curves observed in Figure 3 and Figure 4.
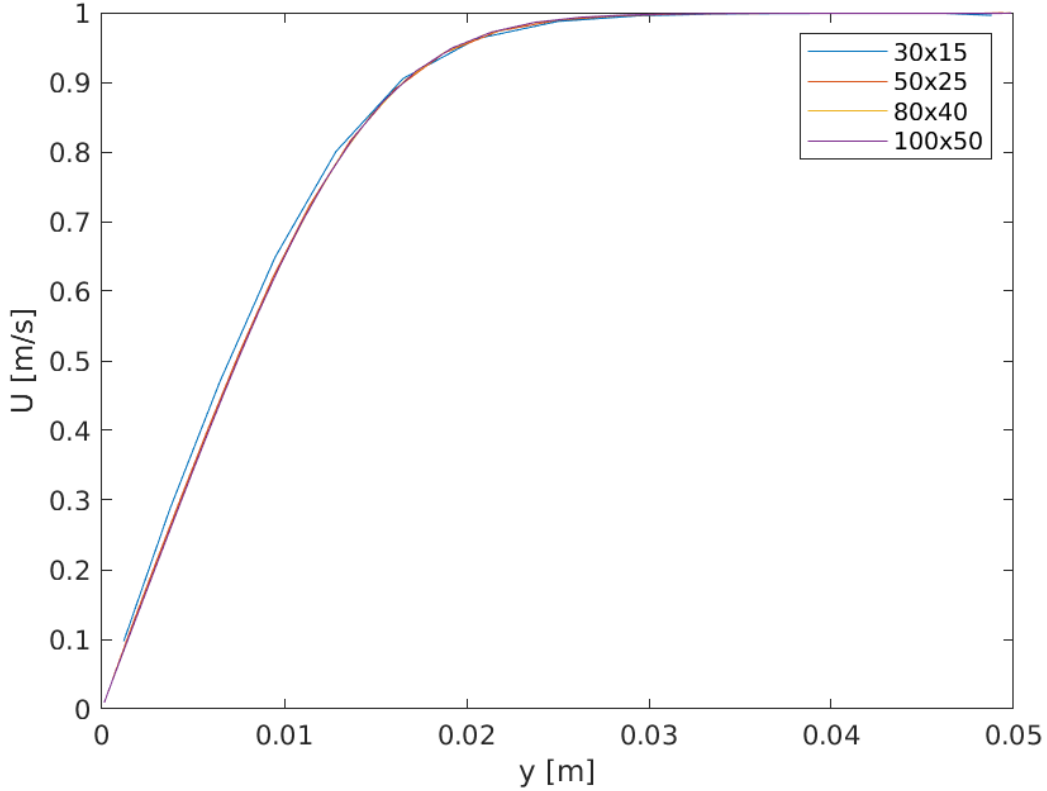

Figure 3: X-velocity grid-independence study

Once grid-independence was confirmed, we decided to use the most refined configuration (100x40 cells in region of study).

3   Comparison against the Blasius solution

Before comparing the results to the theoretical model, we first verified that the CFD solution was self-similar; i.e., that the vertical profiles of the normal-
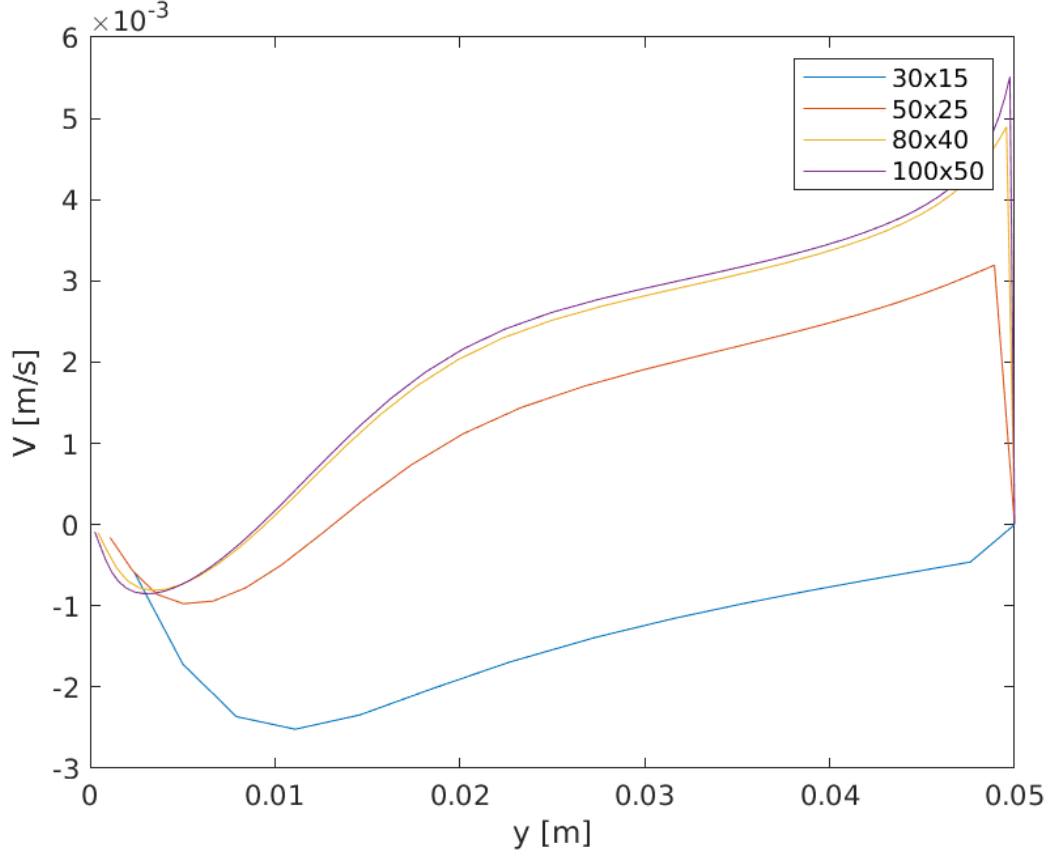
Figure 4: Y-velocity grid-independence study

ized horizontal velocity $\frac{u(x,y)}{U_\infty}$ and the normalized vertical velocity $\frac{v(x,y)}{U_\infty}\sqrt{\frac{U_\infty x}{\nu}}$ collapsed over each other throughout the channel (i.e., for different values of x) when expressed as a function of $\eta = y\sqrt{\frac{U_\infty}{\nu x}}$. Once this property was verified, we added to each set of curves the theoretical solution for the normalized velocity profiles as functions of η, given by the expressions in Equation 1 and 2, based on the value for $f(\eta)$ and $f'(\eta)$ found in Table 1. The results of this procedure can be observed in Figure 5 and Figure 6 respectively.

$$\frac{u}{U_\infty} = f'(\eta) \tag{1}$$

$$\frac{v}{U_\infty}\sqrt{\frac{U_\infty x}{\nu}} = \frac{1}{2}[\eta f'(\eta) - f(\eta)] \tag{2}$$

η	$f(\eta)$	$f'(\eta)$
0	0	0
0.4	0.026	0.133
1	0.1655	0.3298
1.4	0.323	0.4563
2	0.65	0.63
2.4	0.992	0.7289
3	1.397	0.846
3.4	1.7469	0.9017
4	2.305	0.956
4.4	2.692	0.8758
5	3.283	0.992
6	4.279	0.998
7	5.279	0.999

Table 1: Blasius solution reference function

In order to analyze the Skin-friction coefficient profile, we extracted the simulated valuue of this variable as a function of the vertical derivative of the horizontal velocity, making use of the expression in Equation 3. Then, we calculated the model's value as a function of the normalized Reynolds-normalized horizontal axis $\mathrm{Re}_x = \frac{xU_\infty}{\nu}$ using Equation 4.

Using Re_x as independent variable, we plotted both curves in Figure 7; as we can observe, both profiles are identical to a point where the differences can be atributed to numerical error. This trend was sustained throughout the analysis of the subsequent 3 profiles.

$$C_f = \frac{\mu}{\frac{1}{2}\rho U_\infty^2}\frac{\partial u}{\partial y} \tag{3}$$
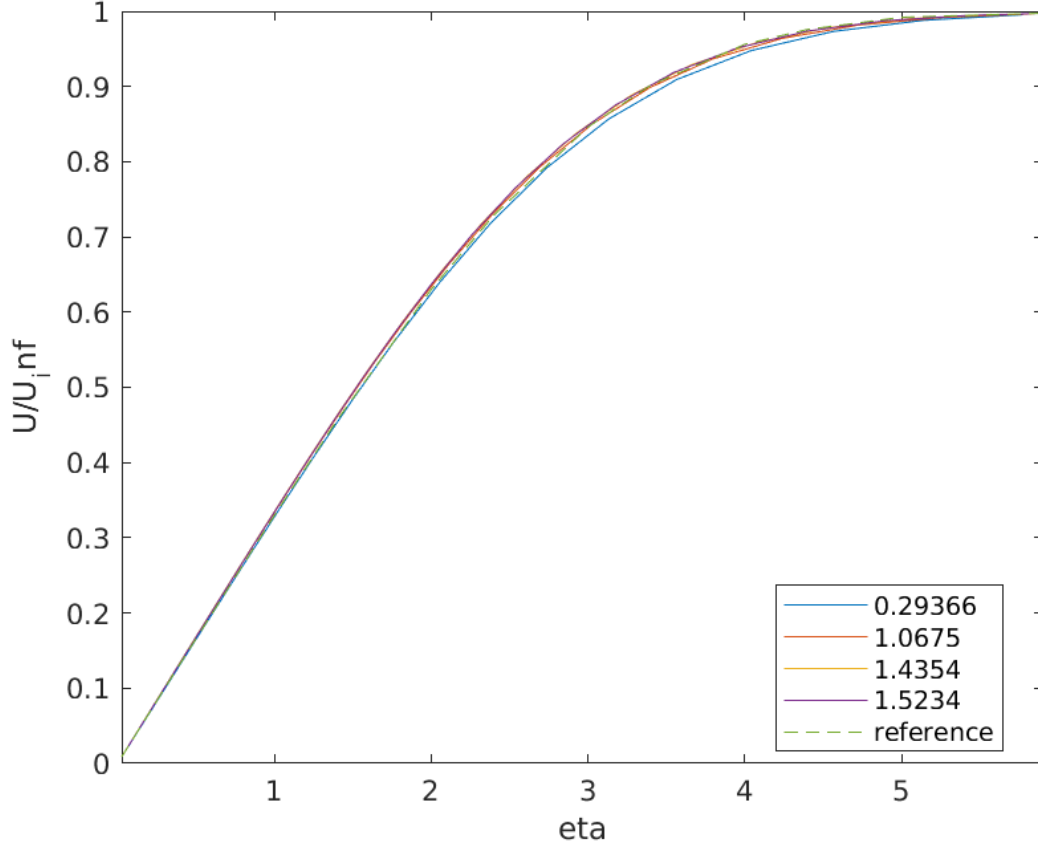
$$C_f = 0.664\sqrt{\mathrm{Re}_x} \tag{4}$$

Figure 5: Normalized X-velocity profile self-similarity

3.1 Boundary Layer Thickness

The CFD value for the Boundary Layer Thickness was obtained by looking up, for every value of x inside the channel, the smallest value of y s.t. $u(x, y) \geq 0.99 U_\infty$ and then divided said value by x. We then calculated the Blasius solution as indicated by Equation 5.

The resulting profiles were then plotted against the independent variable Re_x, as it can be observed in Figure 8.

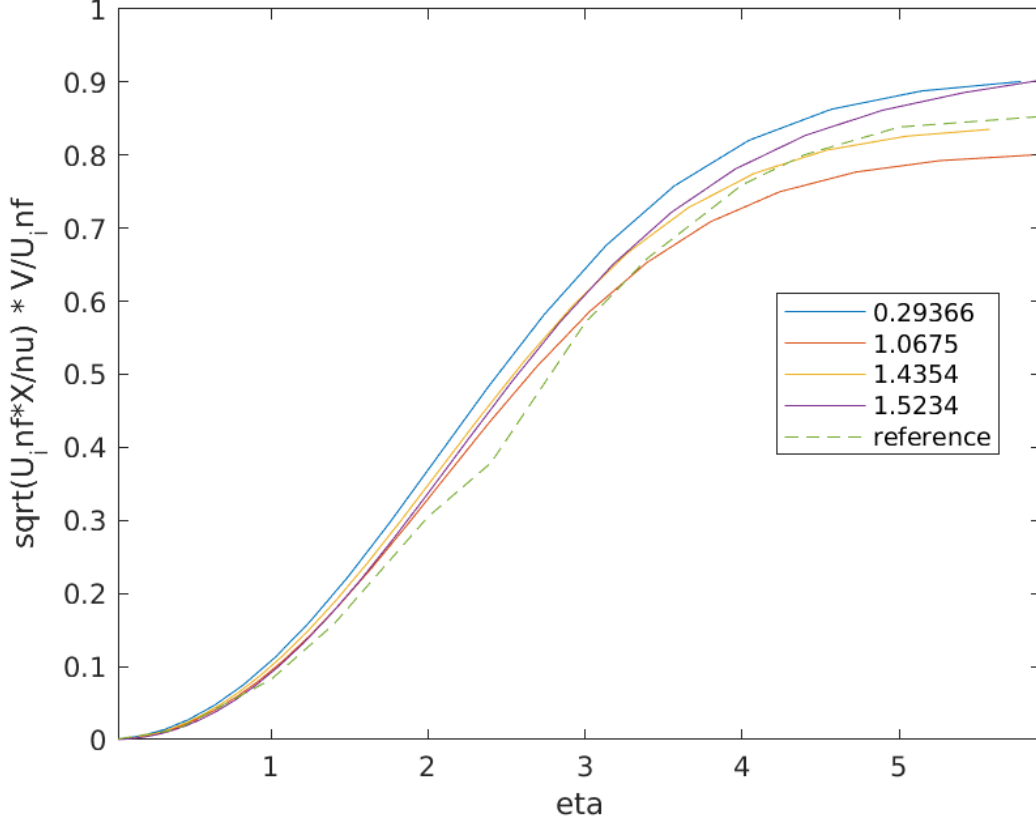$$\frac{\delta(x)}{x} = 5\mathrm{Re}_x^{-\frac{1}{2}} \tag{5}$$

8

Figure 6: Normalized Y-velocity profile self-similarity

3.2 Boundary Layer Thickness

The CFD value for the Displacement Thickness was obtained by integrating
the remainder of the ratio between the instantaneous horizontal velocity and
the uniform velocity through each section of the channel, and then normal-
izing by x (as in Equation 6). We then calculated the Blasius solution as
indicated by Equation 7.

   The resulting profiles were then plotted against the independent variable
Re_x, as it can be observed in Figure 9.

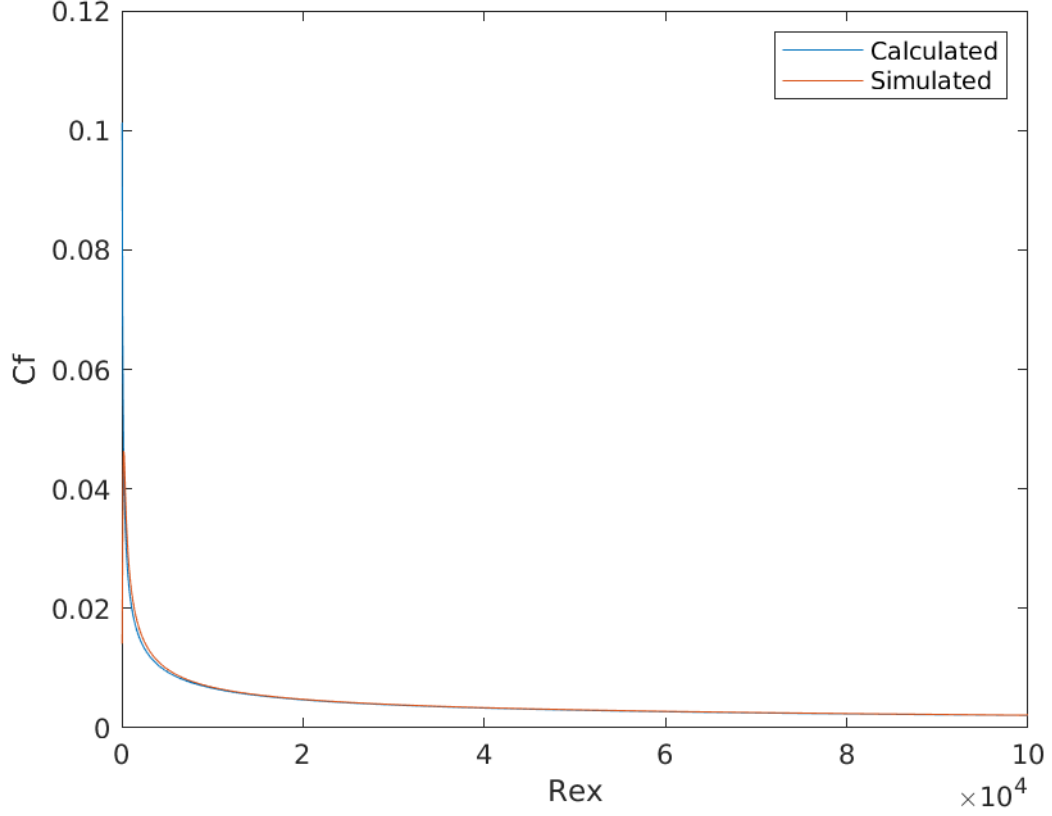$$\frac{\delta^*(x)}{x} = \frac{\int_0^\infty (1 - \frac{u}{U_\infty})dy}{x} \tag{6}$$

9

Figure 7: Skin-friction coefficient profiles

$$\frac{\delta^*(x)}{x} = 1.7208 \mathrm{Re}_x^{-\frac{1}{2}} \tag{7}$$

3.3 Boundary Layer Thickness

The CFD value for the Momentum Thickness was obtained by integrating the remainder of the ratio between the instantaneous horizontal velocity and the uniform velocity multiplied by said ratio through each section of the channel, and then normalizing by x (as in Equation 8). We then calculated the Blasius solution as indicated by Equation 9.

The resulting profiles were then plotted against the independent variable Re_x, as it can be observed in Figure 9.
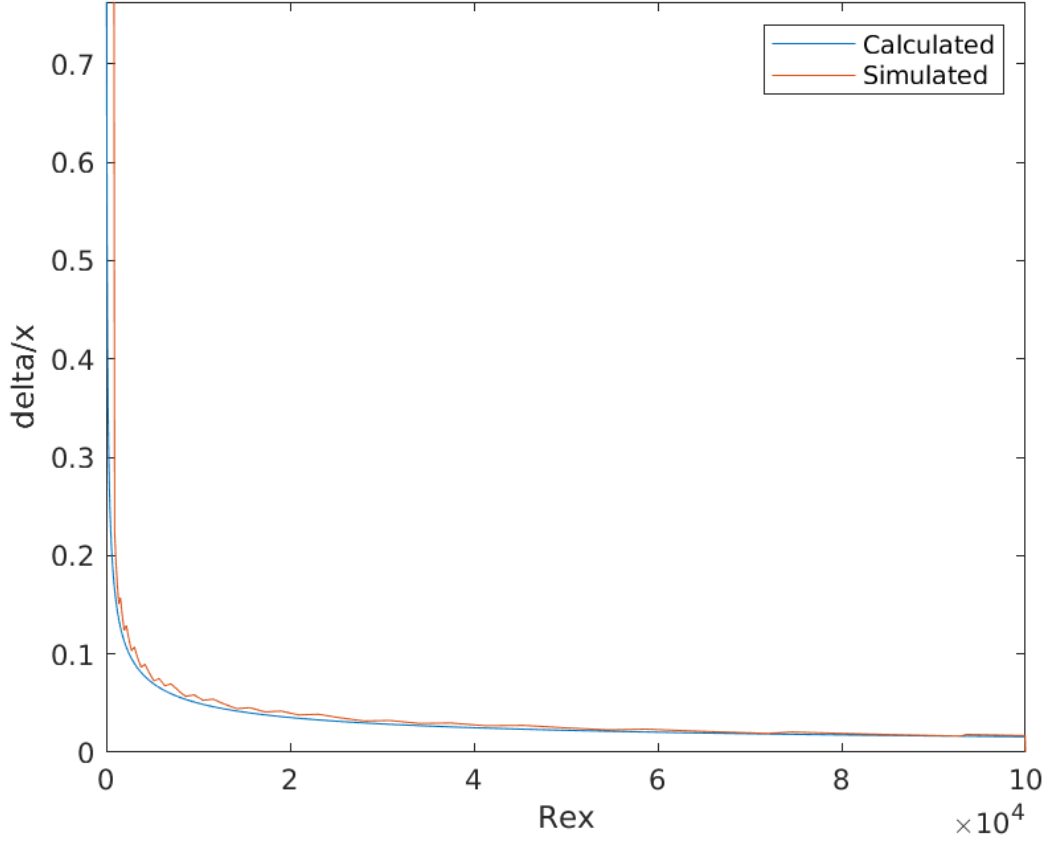
10

Figure 8: Boundary Layer Thickness profiles

$$\frac{\Theta(x)}{x} = \frac{\int_0^\infty \frac{u}{U_\infty}(1 - \frac{u}{U_\infty})dy}{x} \tag{8}$$

$$\frac{\Theta(x)}{x} = 0.664\mathrm{Re}_x^{-\frac{1}{2}} \tag{9}$$

References

[1] Prof. G. V. Messa and Dr. G. Ferrarese. Test case 3: Development of boundary layer over a flat plate. Lab Guide, Fluid Labs, 2021.
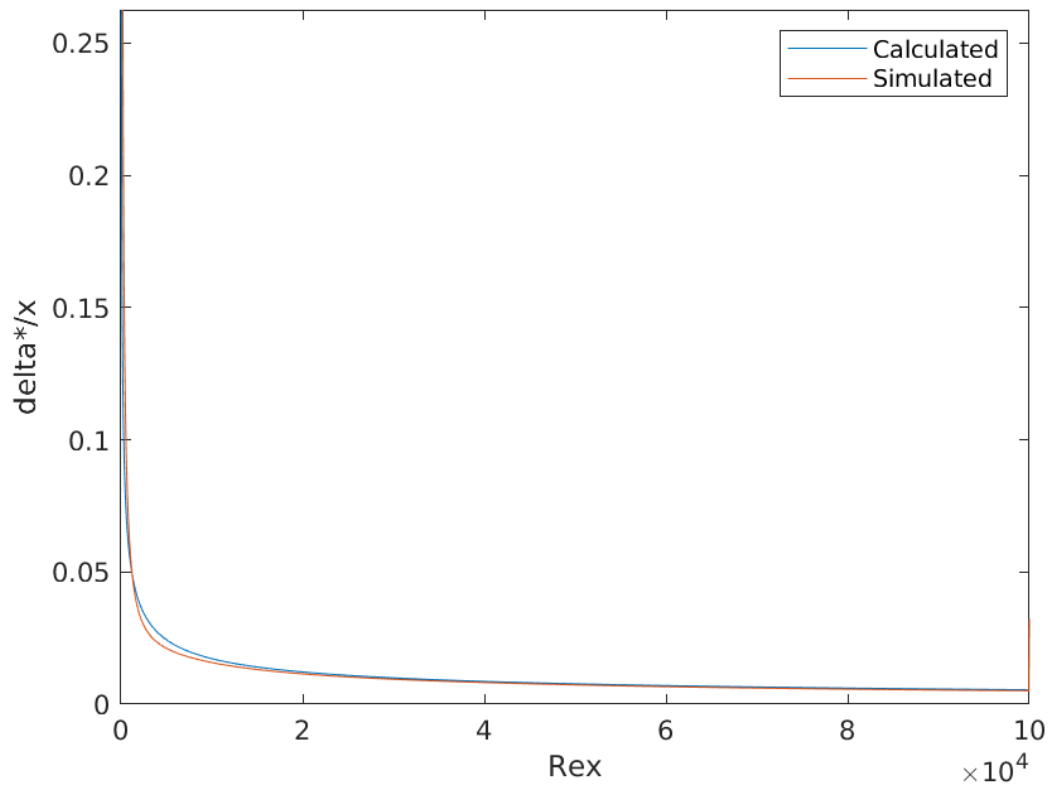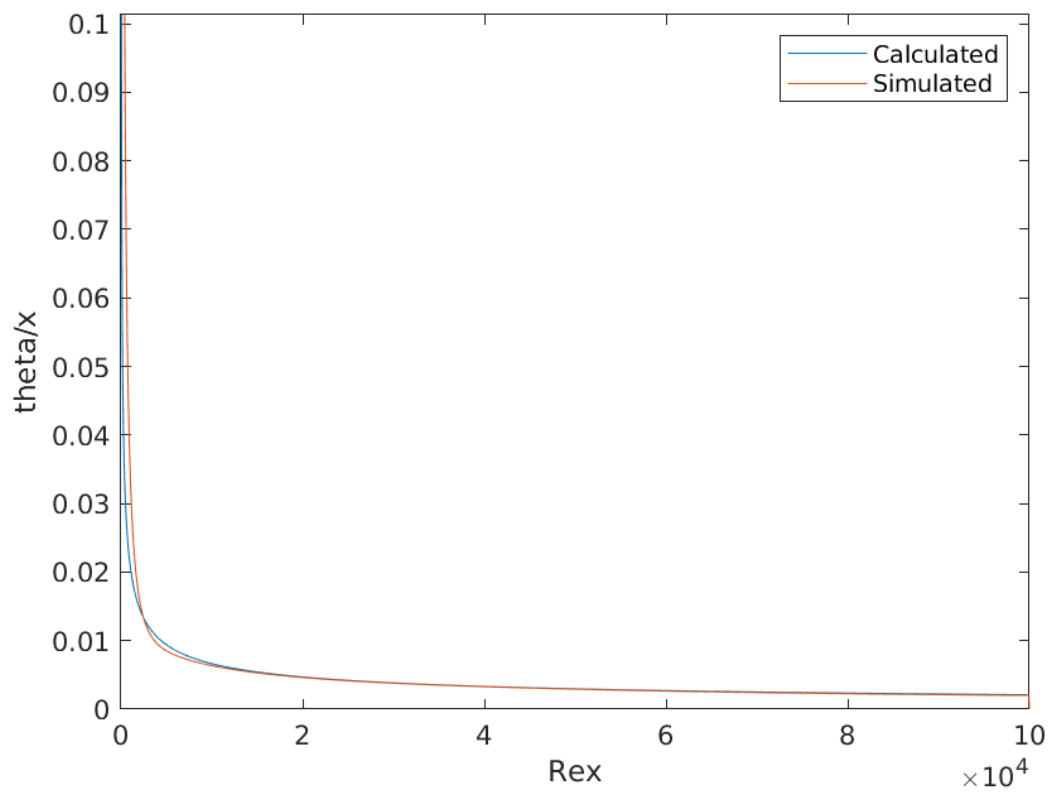
Figure 9: Displacement Thickness profiles

Figure 10: Momentum Thickness profiles